Available online at www.sciencedirect.com

ScienceDirect

Physics Procedia 5 (2010) 203–211

Physics Procedia

www.elsevier.com/locate/procedia

LANE 2010

Fabrication of periodic nano-hole array on GaN surface by fs laser for improvement of extraction efficiency in blue LED

Seisuke Nakashima[a]*, Koji Sugioka[a], Takuma Ito[a, b], Hiroshi Takai[b], and Katsumi Midorikawa[a]

[a]*RIKEN – Advanced Research Institute, 2-1 Hirosawa, Wako-shi, Saitama 351-0198, Japan*
[b]*Tokyo Denki University, 2-2 Nishiki-machi, Kanda, Chiyoda-ku, Tokyo 101-0054, Japan*

Invited Paper

Abstract

For micro/nanofabrication of Gallium nitride (GaN), we developed wet-chemical-assisted femtosecond-laser ablation method. Obtained ablation craters exhibit higher quality and better uniformity without residual debris compared with those produced by femtosecond-laser ablation in air followed by etching. Multi-scan irradiation was performed to fabricate periodic structure composed of high aspect ratio nano-holes using the wet-chemical-assisted ablation method. The aspect ratio is much improved (~1.6) compared to the case of using single pulse irradiation. This periodic structure of uniform nano-holls arranged on GaN surface can act as a two-dimensional photonic crystal which is expected to enhance a light extraction efficiency of blue LED.

Keywords: Femtosecond laser; Wet-chemical process; Gallium nitride; Nano-fabrication; Laser ablation; Periodic structure

1. Introduction

Wide band-gap gallium nitride (GaN) is one of the most promising key materials for various optical devices in blue or ultraviolet region, as typified by light emitting diodes (LED) and laser diodes. In the near future, highly-efficient fabrications of GaN in micro- or nanometer order will become necessarily important techniques for advanced application of GaN based optical devices. Due to high chemical durability and high hardness, however, it is difficult to fabricate GaN based materials with high efficiency for mass production. In case of conventional semiconductors, such as Si and GaAs, electron beam lithography processes followed by dry plasma etching [1-6] are generally utilized as existing techniques. In a meanwhile, our group has demonstrated an availability of laser ablation techniques. In this work, we found that the fabrication efficiency can be improved by using high power KrF excimer laser, F_2 laser [7-9] or multiwavelength (KrF and F_2) laser ablation techniques [10-12]. Although these

* Corresponding author. Tel.: +81-48-462-1111(8544); fax: +81-48-462-4682.
E-mail address: seisuke@riken.jp.

1875-3892
doi:10.1016/j.phpro.2010.08.138

methods are capable of performing high–quality ablation with little thermal damage, it is almost impossible to form three-dimensional (3D) microstructures or high aspect ratio nanostructures, since they are based on single-photon absorption. Because of recent increasing demands for complicated nanostructures of GaN, we adopted a femtosecond (fs) laser process, which is widely used for performing 3D microfabrication [13-15]. The peak intensity of a focused fs-laser beam is so high that multiphoton absorption occurs in a localized region around the focal point, even inside transparent materials. In addition, multiphoton absorption can induce many processes, including ablation, electron excitation, ionization, and phase transitions. Since the fs laser ablation is direct and simple process compared to a variety of lithography techniques, this method could be developed as a novel fabrication technology with high efficiency and high throughput for mass production. In this paper, we investigated the possibility of nanoscale fabrication of GaN by using a reduced effective spot size due to multiphoton absorption, and also tried to improve the fabrication resolution using the second harmonic of near infrared fs laser.

As future prospects of this technique, we can propose some practical applications with 3D or two-dimensional (2D) micro- or nanostructures. One example is 3D hollow channels inside GaN substrates, which is potentially useful for a variety of integrated microfluidic devices. Meanwhile, this fs-laser ablation technique can be applied to formation of 2D photonic crystal (PhC) structures on LED surfaces, in which high aspect ratio and nano-sized air holes are arranged periodically. Because GaN has a high refractive index (n~2.5) compared to air (n~1), only a small part of light generated inside GaN based LED can go out of devices due to total internal reflection. Recently, it has been expected that an external quantum efficiency of blue LEDs will be enhanced by texturing this kind of PhC patterns on top of devices [16-18]. To fabricate 2D photonic crystals on devices, electron beam lithography followed by plasma etching processes are utilized as existing technologies [19, 20]. This method, however, provides high cost and low throughput due to complicated processes. At the last of this paper, we tried to fabricate simple 2D photonic crystals composed of high aspect ratio nanosized holes using the wet-chemical-assisted fs laser ablation method. In order to realize high aspect ratio, the multi-scan irradiation with pulse-controlled fs-laser was carried out.

2. Experimental

Single-crystal n-type GaN substrate in (0001) orientation was utilized in this work, which is commercially available (Kyma Technologies, Inc.) and 470 μm thick. We carried out an irradiation with fs laser in air followed by HCl acid solution etching for 1 hour. Hereafter, this process is referred to as the "two-step processing method. The fs laser (Clark-MXR, CPA-2001) emits pulses with pulse widths of 150 fs [full width at half maximum (FWHM)], a wavelength of 775 nm (fundamental) and 387 nm (SHG) produced by a BBO crystal, and a repetition rate of 1 kHz. The laser beam was shaped by an aperture to a diameter of 3 mm and was focused onto the surface of GaN substrate in air. The focusing lenses are ×20 microscope objective lens for fundamental wavelength with a numerical aperture (NA) of 0.46 and a ×39 microscope objective lens for SHG light with an NA of 0.5. The substrate was translated using a PC-controlled xyz stage with a positioning resolution of 0.5 μm. We also performed wet-chemical-assisted fs laser ablation method. The laser beam was directly focused on the surface of GaN substrate immersed in acid solution. A protective cover glass with the average thickness of 150 μm was put above the GaN substrate and the space between the cover glass and substrate was filled with 35 % concentrated HCl acid solution, the distance of which is about 600 μm. The fabricated structures were investigated by atomic force microscopy (AFM) and optical microscopy. Cross-sectional profiles were also derived from the AFM data, leading to measurements of depths and FWHM diameters for each crater. Changes in chemical composition in the ablated region were examined by X-ray photoelectron spectroscopy (XPS).

3. Results and discussion

3.1. Ablation craters formed by single pulse irradiation

Figure 1 shows structures and cross-sectional profiles of typical ablation craters formed on the GaN surface by the two-step processing method. Each crater was formed by a single shot of fs-laser beam. The pulse energy of the fs

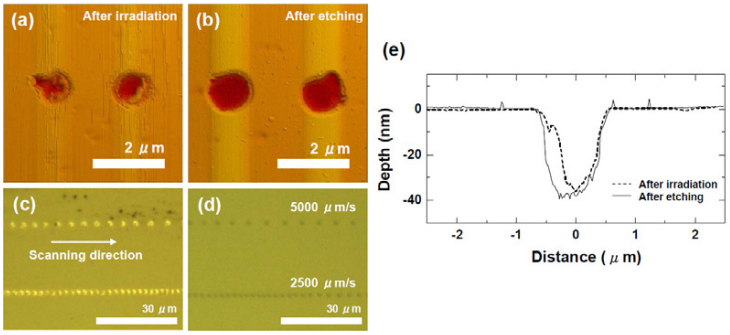

Fig. 1. AFM images of ablation craters formed on GaN surfaces (a) after irradiation and (b) after etching in 35 % HCl solution. Optical microscope images (c) after irradiation and (d) after etching in 35 % HCl solution. (e) Cross-sectional profiles of craters before and after etching.

laser was 80 nJ. As shown in Fig. 1(a), the roughness of ablated surface is quite high and the edge of crater is ambiguous due to residual debris. Successive etching in concentrated HCl solution removed some of the debris. Although the edge became better, the roughness was just slightly improved (Fig. 1 (b)). Figures 1 (c) and (d) show optical micrographs taken before and after etching, respectively. The irradiated spots before etching appear bright due to high reflectivity. After etching, that region turned into dark, indicating that the highly reflective phase was removed by HCl etching. As clearly seen in the cross-sectional profiles in Fig. 1(e), a layer was removed after etching. These results can be explained in terms of a Ga-rich phase with metallic high reflectivity, which was formed on the surface of craters by irradiation with a fs laser pulse [7] and was etched by HCl acid solution. A measurement of change of chemical compositions by XPS supports the prediction about an existence of Ga-rich phase [21]. At the first step, a direct ablation process takes place near the focal point, in which the laser intensity exceeds the ablation threshold. And also a dissociation reaction of Ga-N bonds occurs, in which the laser intensity is less than the ablation threshold, resulting in a formation of Ga-rich layer. In the second step, the HCl etching dissolves these metallic Ga-rich phases.

Figures 2 (a) and (b) show AFM images of ablation craters produced by wet-chemical-assisted fs-laser ablation in a 12 mol/l HCl solution for pulse energies of 53 and 105 nJ, respectively. Compared with the case of the two-step processing method, ablation craters are more symmetrical with clear edge. The results by wet-chemical-assisted ablation using 1.2 and 0.12 mol/l HCl are also exhibited in Figs. 2 (c) and 3 (d), respectively. In lower concentrations, more debris still remains, resulting in lower quality ablation compared with the case of concentrated HCl solution. Figure 3 compares cross-sectional profiles of craters between (a) two-step processing and (b) wet-chemical-assisted fs-laser ablation. As increasing the pulse energy, it is found that the bottom surface of crater

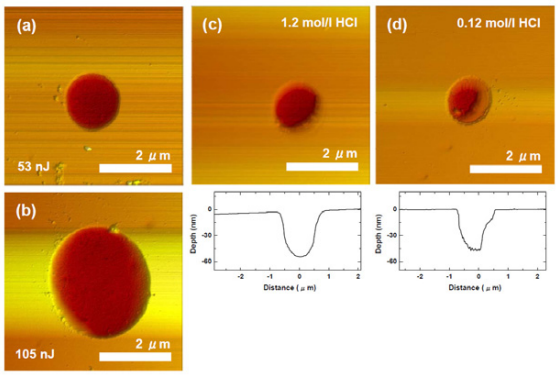

Fig. 2. Surface topographies of ablation craters formed at pulse energies of (a) 53 and (b) 103 nJ by wet-chemical-assisted fs-laser ablation. AFM images of ablation craters fabricated by wet-chemical-assisted fs-laser ablation using (a) 3.5 and (b) 0.35 % HCl solution.

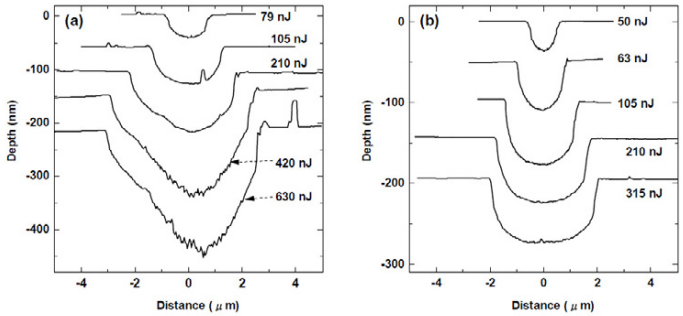

Fig. 3. Cross-sectional profiles of ablation craters formed by (a) two-step processing method and (b) wet-chemical-assisted fs-laser ablation.

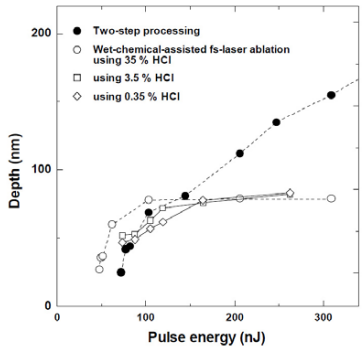

Fig. 4. Dependences of etching depth on pulse energy for two-step processing method (●) and for wet-chemical-assisted fs-laser ablation in 35 (○), 3.5 (□) and 0.35 (◊) % HCl solution.

formed by two-step processing becomes rougher than that produced by wet-chemical-assisted fs-laser ablation. The wet-chemical-assisted ablation process is basically similar to that of two-step processing; direct ablation with formation of Ga-rich phase, and etching of the phase by HCl acid solution. However, despite there being no individual etching step in HCl solution, the debris is almost completely removed in contrast to the two-step processing method. It is presumed that Ga-rich phase and ablation debris are effectively removed due to a diffusion effect in HCl solution. Figure 4 shows the variation of ablation depth as a function of pulse energy for two methods. It is notable that the minimum energy for wet-chemical-assisted ablation is lower than that for two-step processing. Moreover, the minimum energy for ablation increases as the decrease in the concentration of the HCl solution. It is speculated that wet-chemical-assisted ablation contains a photochemical or photothermal process due to immersion effect in HCl solution. We also find the saturation tendency of etch depth at higher pulse energy for wet-chemical-assisted ablation. This is the reason why the craters' bottom becomes flat as seen in Fig. 3(b), and will be discussed at the next Section. Consequently, the HCl solution evidently plays an important role in the great improvement in ablation quality.

3.2. Enhancement of fabrication resolution

Nanoscale fabrication for GaN is of great interest because of the potential application to a variety of micro- or nanodevices. In the previous chapter, a 1.3-μm-diameter crater was formed by single-pulse irradiation with a pulse energy of 80 nJ using two-step processing method. Meanwhile, by using wet-chemical-assisted fs-laser ablation, an ablation crater with a diameter of 1.1 μm can be produced at a pulse energy of 47 nJ. These results suggest that wet-chemical-assisted ablation can provide higher resolution than the other method, which is presumably due to a

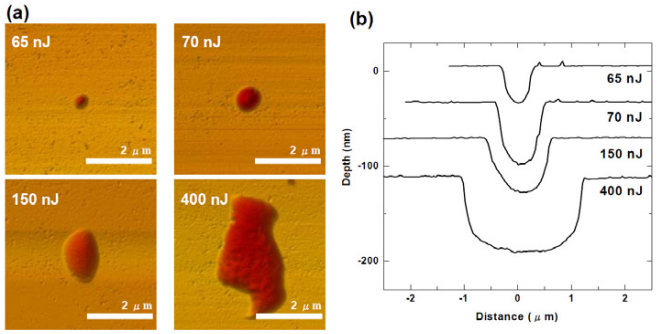

Fig. 5. (a) AFM images and (b) cross-section profiles of ablation craters formed by a wet-chemical-assisted fs laser ablation in 35% HCl acid solution.

cooling effect of liquid solution. This effect can be discussed as follows. The Ga-rich layer is formed in regions where the beam fluence is less than the ablation threshold fluence. Since the heat conductivity of liquid solution is higher than that of air, some part of thermal energy generated by irradiation transfers into the HCl solution. Consequently, the thickness of a Ga-rich layer decreases, resulting in small etched region, namely high-resolution fabrication.

Generally, selecting a shorter wavelength is an effective way to enhance the fabrication resolution due to smaller spot size of a laser beam. We utilize a second harmonic of near infrared fs laser (λ= 387 nm) for wet-chemical-assisted fs-laser ablation method. Figure 5 (a) shows AFM images for the pulse energies of 65, 70, 150, and 400 nJ using a 35 % concentrated HCl acid solution. At the pulse energy lower than 70 nJ, high quality ablation craters with better round shape are obtained, in which the ablation debris is well removed by the concentrated HCl solution. In Fig. 5 (b), cross-sectional profiles also illustrate the smoothness of craters' surface. An ablation crater as small as 320 nm is successfully fabricated at the pulse energy of 65 nJ, which is the minimum energy for fabrication of craters. This fabrication resolution is higher than the case of using fundamental light of near-infrared fs laser as described above. In the pulse energy higher than 250 nJ, the ablation craters change from symmetrical round to ellipsoidal shape. This is ascribable to the fact that the incident pulse is interfered or scattered by ablation bubbles generated from the preceding pulse, because such distortion was not observed in the case of ablation in air. Figure 6 shows the variation in crater depth as a function of pulse energy. The depth of ablation craters tends to be saturated at 80 nm, suggesting that the ablation process is due to multi-photon absorption. Band gap of the GaN is 3.4 eV, which is so large that a single photon of SHG light is unable to excite an electron from the valence band to the conduction band. Therefore, it is predicted that the ablation reaction takes place by two-photon absorption. When an ablation crater with a depth of X nm was formed on a GaN surface by an irradiation with focused fs laser, the propagated laser intensity at the depth of X corresponds to the threshold intensity of ablation, I_{th}, and the depth of ablation craters is expressed by

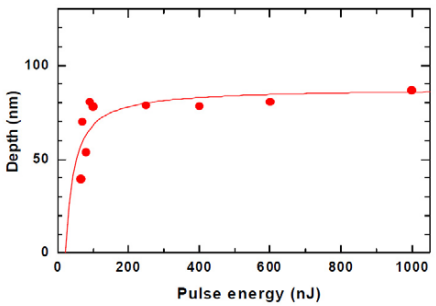

Fig. 6. Variation in crater depth as a function of pulse energy for concentrated HCl acid. Solid line is a fit with the Equation 1 based on optical absorption due to two-photon absorption.

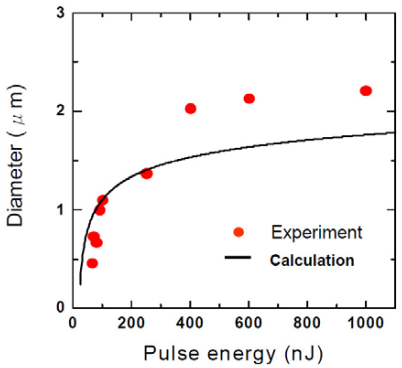

Fig. 7. Calculated diameter of ablation craters as a function of pulse energy for concentrated HCl solution. Red circles represent experimental data.

$$X = \frac{1}{\alpha}\left(\frac{1}{I_{th}} - \frac{1}{I_0}\right), \tag{1}$$

where α is a nonlinear absorption coefficient. From a fit of this equation to the experimental depth data (solid line in Figure 3), I_{th} for ablation of GaN due to two-photon absorption is estimated as 3.60×10^{13} W/cm^2. By the way, a beam profile of fs laser is expressed using Gaussian function as;

$$I(r) = I_0 \exp\left(-\frac{2r^2}{\omega_0^{\,2}}\right), \tag{2}$$

where r represents a distance from the center of beam and $I(r)$ represents the intensity in this position. Gaussian beam radius ω_0 was estimated as 0.64 μm by an equation of $\omega_0 = 0.61\cdot\lambda / NA\cdot M^2$. Here, M^2 for our fs-laser system is 1.3, NA = 0.5 and λ = 0.387 μm. Converting the incident laser intensity I_0 into the total pulse energy P by an equation of $I_0 = 2\cdot P/\left(\tau_p\cdot\pi\omega_0^{\,2}\right)$, $I(r)$ can be expressed using P as;

$$I(r) = \frac{2P}{\tau_p\cdot\pi\omega_0^{\,2}}\exp\left(-\frac{2r^2}{\omega_0^{\,2}}\right). \tag{3}$$

Since only the region where the laser intensity exceeds I_{th} should be ablated, a theoretical diameter of ablation crater, D (= $2r(I_{th})$) associated with I_{th} can be calculated by

$$D = 2r_{th} = \omega_0\sqrt{\ln\left(\frac{2P}{\tau_p\cdot\pi\omega_0^{\,2}I_{th}}\right)}. \tag{4}$$

In Fig. 7, a theoretical curve of ablation diameter calculated for various pulse energies (solid line) is shown with the experimental data of diameter denoted by red closed circles. The calculation is in accordance with the experimental values in the region of energy lower than 250 nJ. By contrast, in the region of energy higher than 400 nJ, calculated diameters are underestimated compared to the experimental data. At present, we speculate that this discrepancy is probably due to effect of thermal diffusion or to the distortion of beam shape interfered by bubbles as discussed before.

3.3. High aspect ratio nano-holes formed by multi-scan irradiation

For application to 2D photonic crystal structures on LED, we tried to fabricate high aspect ratio nano-holes using wet-chemical-assisted ablation method. By scanning the focal point of fs laser, we arranged two-dimensional periodical array of nano craters by single pulse ablation. However, there are two critical problems. One is low

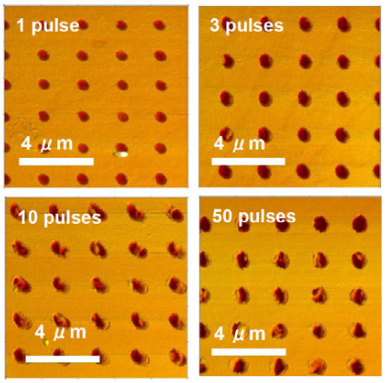

Fig. 8. AFM images of nano-hole arrays formed by multi-scan irradiation with 1, 3, 10, 50 pulses, respectively.

positioning accuracy of stage with stepping motors. Therefore, we utilized a highly accurate piezo stage for the scanning and a pulse picker to control the repetition rate of fs laser. Due to the synchronization of the stage with laser pulse, the position of pulse irradiation was successfully controlled, resulting in highly periodic arrangement of nano-holes. The second issue is that higher aspect ratio nano-holes are required to enhance extraction efficiency. In the case of using single pulse irradiation, however, the depth of crater is saturated at higher pulse energy, while the diameter increases as stated above. As a result, the aspect ratio is limited to about 0.2 at highest. According to some experimental results or a FDTD simulation, the aspect ratio needs to be higher than 1.5. Then, we propose that multi-pulse ablation is an effective way of obtaining higher aspect ratio nano-holes. One of the easiest methods is successive multi-pulse irradiation. By changing the open time of shutter, the pulse number can be controlled. However, when the ablation reaction occurs inside solution, namely, wet-chemical-assisted ablation, the micro-bubble generated by the preceding pulses interferes the following pulses, resulting in quite low fabrication efficiency. If the time interval between pulses is longer than the time scale for disappearing of bubbles, namely using a low repetition rate, the interference by bubble would be minimal. At the same time, the fabrication time become much longer. To avoid this micro-bubble effect, we developed a multi-scan irradiation technique, in which a scanning with single pulse irradiation is repeated at each spot. This method need not decrease the repetition rate. In addition, a thermal accumulation would be minimized. Figure 8 shows AFM images of nano-hole array formed by multi-scan irradiation using wet-chemical assisted ablation in HCl solution. The scanning number, namely, pulse number was 1, 3, 10 and 50 pulses, respectively. It is found that overlapping of repeated pulse position is well controlled at each spot, which is due to high positioning accuracy of piezo stage. In Figure 9 is shown the variations of diameter and depth as a function of pulse number. The diameter does not change so much as the increase in the pulse number.

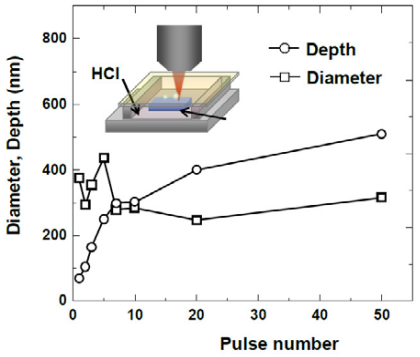

Fig. 9. Variation of diameter and depth of nano-holes formed by wet-chemical-assisted ablation method as a function of pulse number.

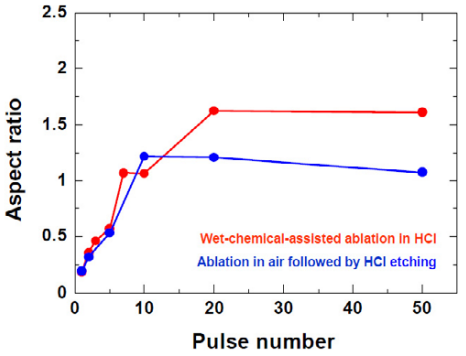

Fig. 10. Variation of aspect ratios of nano-holes formed by wet-chemical-assisted ablation and by two-step processing method as a function of pulse number.

Meanwhile, the depth has a tendency to increase below 20 pulses, and the value is saturated for higher pulse numbers. In Figure 10, the variations of aspect ratio as a function of pulse number are plotted. We also performed multi-scan irradiation using the two-step processing method for comparison. As increasing the pulse number, aspect ratios for each method increase and are saturated at around 10 or 20 pulses. The saturated ratios are 1.6 for the wet-chemical-assisted ablation and 1.2 for the two-step processing, respectively. These values are much higher than the aspect ratio in the case of single pulse ablation. More notable is the fact that the saturated value for wet-chemical-assisted ablation is 30 % higher than that for ablation in air.

Basically, in the multi-scan irradiation, a wet-chemical-assisted ablation process by single pulse is repeated with sufficient time interval for disappearance of bubbles or removal of debris. After 20 pulses, this ablation process no longer occurs, because the beam intensity at the bottom is smaller than the threshold intensity of ablation. In other words, the bottom of craters reached to the limit of focus depth. Therefore, it is speculated that final shape of ablation crater is determined by the spatial intensity distribution of laser beam. Given an *r*-*z* coordinate space, a laser beam is irradiated in *z* direction and focused at the point of origin. If the intensity distribution of incident laser is described as a Gaussian, the intensity at arbitrary coordinate point, $I(r, z)$ can be derived from Equation (2) as

$$I(r,z) = I_0(z)\exp\left(-\frac{2r^2}{\omega(z)^2}\right), \tag{5}$$

where $I_0(z)$ denotes an intensity at center of beam and $\omega(z)$ represents a beam radius. Then, given an optional beam intensity I_O, the relationship between z and r can be obtained, leading to closed isointensity curves for various optional beam intensities. If the optional intensity is set to the threshold intensity I_{th}, the obtained isointensity curve represents ablated region by multi-scan irradiation method as

$$r^2 = -\frac{\omega(z)^2}{2}\ln\frac{I_{th}}{I_0(z)}. \tag{6}$$

In this case, the depth Z_{th} and radius r_{th} of ablation craters are estimated as

$$Z_{th} = \frac{\pi\omega_0^2 n}{\lambda}\sqrt{\frac{2I_0}{\pi\omega_0^2 I_{th}} - 1}, \tag{7}$$

and

$$r_{th} = \omega_0\sqrt{-\frac{1}{2}\ln\frac{\pi\omega_0^2 I_{th}}{2I_0}}. \tag{8}$$

It is interesting to note that the depth depends on a refractive index of medium faced with GaN substrate, n. Meanwhile, the radius is independent of the refractive index. As a result, the aspect ratio will depend on the refractive index of medium. The difference in refractive index between air and HCl acid solution of 1.3, it is concluded that the aspect ratio for wet-chemical assisted ablation method is about 30 % higher than that for simple dry ablation process. This estimation agrees well with the experimental results.

4. Conclusions

We have investigated the effectiveness of micro- or nano-machining for the wide-bandgap semiconductor GaN by using fs-laser ablation process. We developed a wet-chemical-assisted fs-laser ablation technique, in which the laser beam is directly focused on surface of GaN substrate immersed in HCl acid solution. High quality ablation crater was fabricated without residual debris. We also performed a conventional laser ablation in air followed by HCl etching (two-step processing method) to create ablation craters. The structures of obtained craters exhibit lower quality than the wet-chemical-assisted ablation method. At the first step, direct ablation with formation of Ga-rich phase occurs, and the phase was etched by HCl acid solution at the second step. Although these two processes simultaneously occur in the wet-chemical-assisted ablation method, the combined and simplified ablation technique successfully made it possible to fabricate high quality ablation craters at shorter processing time. This is due to a photochemical or photothermal effect involved with HCl acid solution. In terms of realization of high resolution, a wet-chemical assisted ablation method is suitable because of cooling effect of resident HCl acid solution. By using second harmonic light of near infrared fs-laser, nano-sized craters as small as 320 nm in FWHM diameter was successfully formed. Ablation threshold peak intensity is evaluated by assuming that the laser ablation is based on two-photon absorption, and we calculated the theoretical diameter of ablation craters. In lower energy, the calculated diameters are well reproduced by experimental values, while the actual values in the region of higher energy are larger than the estimated values. For the purpose of application to 2D photonic crystal on GaN LED, we also tried to fabricate periodic arrays of high aspect ratio nano-holes on GaN substrates. By controlling the synchronization of piezo-stage with pulse irradiation, almost perfectly periodic array of nano-holes was fabricated on GaN substrate using wet-chemical-assisted fs laser ablation. Periodic array of nano-holes with high aspect ratio (~1.6) was successfully obtained by using multi-scan irradiation method. Final shape of ablation craters formed by multi-scan irradiation is determined by spatial intensity distribution of focused laser beam. It is also found that aspect ratio depends on refractive index of medium faced with GaN substrate.

References

1. S. A. Smith, C. A. Wolden, M. D. Bremser, A. D. Hanhser, R. F. Davis, and W. V. Lampert, Appl. Phys. Lett. 71 (1997) 3631.
2. R. J. Shul, G. B. McClellan, S. A. Casalnuovo, D. J. Rieger, S. J. Pearton, C. Constantine, et al., Appl. Phys. Lett. 69 (1996) 1119.
3. H. P. Gillis, D. A. Choutov, K. P. Matin, S. J. Pearton, and C. R. Abernathy, J. Electrochem. Soc. 143 (1996) L251.
4. H. Lee, D. B. Oberman, and J. S. Harris Jr., Appl. Phys. Lett. 67 (1995) 1754.
5. J. B. Fedison, T. P. Chow, H. Lu, I. B. Vhat, and J. Electrochem. Soc. 144 (1997) L221.
6. D. Basak, M. Verdu, M. T. Montojo, M. J. Sanchez-Garcia, F. J. Sanchez, E. Munoz, and E. Calleja, Semicond. Sci. Technol. 12 (1997) 1654.
7. T. Akane, K. Sugioka, H. Ogino, H. Takai, and K. Midorikawa, Appl. Surf. Sci. 148 (1999) 133.
8. T. Akane, K. Sugioka, and K. Midorikawa, Appl. Phys. A 69 (1999) S309.
9. T. Akane, K. Sugioka, S. Nomura, K. Hammura, N. Aoki, K. Toyoda, et al., Appl. Surf. Sci. 168 (2000) 335.
10. J. Zhang, K. Sugioka, S. Wada, H. Tashiro, K. Toyoda, and K. Midorikawa, Appl. Surf. Sci. 127 (1998) 793.
11. T. Akane, K. Sugioka, K. Hammura, Y. Aoyagi, K. Midorikawa, K. Obata, et al., J. Vac. Sci. Technol. B 19 (2001) 1388.
12. K. Obata, K. Sugioka, K. Midorikawa, T. Inamura, and H. Takai, Appl. Phys. A 82 (2006) 479.
13. K. Miura, J. Qiu, H. Inouye, T. Mitsuyu, K. Hirao: Appl. Phys. Lett. 71 (1997) 3329.
14. Y. Shimotsuma, P. G. Kazansky, J. Qiu, and K. Hirao: Phys. Rev. Lett. 91 (2003) 247405.
15. D. Ashkenasi, G. Müller, A. Rosenfeld, R. Stoian, I.V. Hertel, N.M. Bulgakova, et al., Appl. Phys. A: Mater. Sci. Process. 77 (2003) 223.
16. S. Fan, P. R. Villeneuve, J. D. Joannopoulos, and E. F. Schubert, Phys. Rev. Lett., 78, (1997) 3294.
17. E. Yablonobitch, T. J. Gmitter, and R. Bhat, Phys. Rev. Lett., 61, (1988) 2546.
18. T. N. Oder, H. S. Kim, J. Y. Lin, and H. X. Jiang, Appl. Phys. Lett., 84, (2004) 466.
19. C. Meier, K. Hennessy, E. D. Haberer, R. Sharma, Y.-S. Choi, K. McGroddy, et al., Appl. Phys. Lett., 88, (2006) 031111.
20. K. Kim, J. Choi, S. C. Jeon, J. S. Kim, and H. M. Lee, Appl. Phys. Lett., 90, (2007) 181115.
21. S. Nakashima, K. Sugioka, K. Midorikawa, Applied Surface Science, 255 (2009) 9770.